

One-way quantum computation via manipulation of polarization and momentum qubits in two-photon cluster states

Giuseppe Vallone,* Enrico Pomarico,* Francesco De Martini,* and Paolo Mataloni*
*Dipartimento di Fisica dell'Università "La Sapienza" and Consorzio Nazionale
 Interuniversitario per le Scienze Fisiche della Materia, Roma, 00185 Italy*
 (Dated: November 15, 2018)

Four-qubit cluster states of two photons entangled in polarization and linear momentum have been used to realize a complete set of single qubit rotations and the C-NOT gate for equatorial qubits with high values of fidelity. By the computational equivalence of the two degrees of freedom our result demonstrate the suitability of two photon cluster states for rapid and efficient one-way quantum computing.

PACS numbers: 03.67.Mn, 03.67.Lx

The relevance of cluster states in quantum information and quantum computation (QC) has been emphasized in several papers in recent years [1, 2, 3, 4]. By these states novel significant tests of quantum nonlocality, which are more resistant to noise and show significantly larger deviations from classical bounds can be realized [2, 5, 6, 7]. Besides that, cluster states represent today the basic resource for the realization of a quantum computer operating in the one-way model [1]. In the standard QC approach any quantum algorithm can be realized by a sequence of single qubit rotations and two qubit gates, such as C-NOT and C-Phase [8]. A deterministic one-way QC is based on the initial preparation of entangled qubits in a cluster state, followed by a temporally ordered pattern of single qubit measurements and feed-forward operations. Indeed these operations, depending on the outcome of the measured qubits [1], correspond either to intermediate feed-forward measurements or to Pauli matrix feed-forward corrections on the final output state. Two qubit gates can be realized by exploiting the existing entanglement between qubits. In this way the difficulties of standard QC, related to the implementation of two qubit gates, are transferred to the preparation of the state.

The first experimental results of one-way QC were demonstrated by using 4-photon cluster states [3, 4]. The detection rate in such experiments, approximately 1 Hz, is limited by the fact that four photon events in a standard spontaneous parametric down conversion (SPDC) process are rare. Moreover, four-photon cluster states are characterized by limited values of fidelity, while efficient computation require highly faithful prepared states.

Cluster states at high level of brightness and fidelity were realized by entangling two photons in more degrees of freedom [7]. Precisely, this was demonstrated by entangling the polarization (π) and linear momentum (\mathbf{k}) degrees of freedom of one of the two photons belonging to a hyperentangled state [9, 10]. The high fidelity and detection rate of the prepared two-photon four-qubit cluster states make them suitable for the realization of high speed one-way QC. In this letter we present the realization of arbitrary single qubit rotations and of the

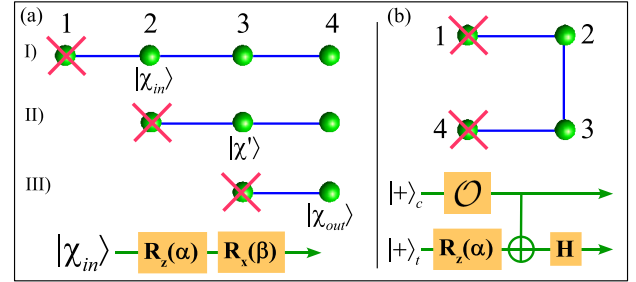


FIG. 1: Measurement pattern for single qubit rotations (a) and C-NOT gate (b). (a) Top: arbitrary single qubit rotations on a four qubit linear cluster state are carried out in three steps (I, II, III). In each measurement, indicated by a red cross, the information travels from left to right. Bottom: equivalent logical circuit. (b) C-NOT gate realization via measurement of qubits 1, 4 on the horseshoe cluster (top) and equivalent circuit (bottom).

C-NOT gate for equatorial qubits. We have also verified the equivalence existing between the two degrees of freedom for qubit rotations, by using either \mathbf{k} or π as output qubit, demonstrating that all four qubits can be adopted for computational applications.

In our experiment two-photon four-qubit cluster states are generated by starting from π - \mathbf{k} hyperentangled photon pairs generated by SPDC process in continuous way. The method to produce the hyperentangled states $|\Xi^{\pm\pm}\rangle = |\Phi^{\pm}\rangle_{\pi} \otimes |\psi^{\pm}\rangle_{\mathbf{k}}$ was explained in other papers [9, 11], to which we refer for details. In the above equations $|\Phi^{\pm}\rangle_{\pi} = \frac{1}{\sqrt{2}}(|H\rangle_A|H\rangle_B \pm |V\rangle_A|V\rangle_B)$, $|\psi^{\pm}\rangle_{\mathbf{k}} = \frac{1}{\sqrt{2}}(|\ell\rangle_A|r\rangle_B \pm |r\rangle_A|\ell\rangle_B)$, H, V correspond to the horizontal (H) and vertical (V) polarizations and ℓ, r refer to the left (ℓ) or right (r) paths of the photon A (Alice) or B (Bob) (see Fig. 1 of [7]).

The cluster state

$$|C_4\rangle = \frac{1}{2}(|H\ell\rangle_A|Hr\rangle_B - |Hr\rangle_A|H\ell\rangle_B + |Vr\rangle_A|V\ell\rangle_B + |V\ell\rangle_A|Vr\rangle_B) \quad (1)$$

is created by starting from the state $|\Xi^{+-}\rangle = |\Phi^+\rangle_\pi \otimes |\psi^-\rangle_{\mathbf{k}}$ and introducing a π phase shift in one of the four output modes of the SPDC source [15]. Precisely, a zero-order half wave (HW) plate is inserted on the r_A mode. This operation, corresponding to a Controlled Phase (CP) between the control (\mathbf{k}_A) and the target (π_A) qubits, create a genuine four-partite entanglement, without any kind of post-selection. Cluster states were observed at 1 kHz detection rate with fidelity $F = 0.880 \pm 0.013$, obtained from the measurement of the stabilizer operators of $|C_4\rangle$ [2].

By using the correspondence $|H\rangle \leftrightarrow |0\rangle$, $|V\rangle \leftrightarrow |1\rangle$, $|\ell\rangle \leftrightarrow |0\rangle$, $|r\rangle \leftrightarrow |1\rangle$, the generated state $|C_4\rangle$ is equivalent to the cluster state $|\Phi_4^{\text{lin}}\rangle = \frac{1}{2}(|+\rangle_1|0\rangle_2|0\rangle_3|+\rangle_4 + |+\rangle_1|0\rangle_2|1\rangle_3|-\rangle_4 + |-\rangle_1|1\rangle_2|0\rangle_3|+\rangle_4 - |-\rangle_1|1\rangle_2|1\rangle_3|-\rangle_4)$ [16] (with $|\pm\rangle = \frac{1}{\sqrt{2}}(|0\rangle \pm |1\rangle)$) up to single qubit unitaries:

$$|C_4\rangle = U_1 \otimes U_2 \otimes U_3 \otimes U_4 |\Phi_4^{\text{lin}}\rangle \equiv \mathcal{U} |\Phi_4^{\text{lin}}\rangle. \quad (2)$$

Here $|\Phi_4^{\text{lin}}\rangle$ and $|C_4\rangle$ are respectively expressed in the so called ‘‘computational’’ and ‘‘laboratory’’ basis, while the U_j 's ($j = 1, \dots, 4$) are products of Hadamard gates $H = \frac{1}{\sqrt{2}}(\sigma_x + \sigma_z)$ and Pauli matrices σ_i . Their explicit expressions depend on the ordering of the four physical qubits, namely \mathbf{k}_A , \mathbf{k}_B , π_A , π_B . In this work we use three different ordering:

- a) $(1,2,3,4) = (\mathbf{k}_B, \mathbf{k}_A, \pi_A, \pi_B)$, $\mathcal{U} = \sigma_x H \otimes \sigma_z \otimes \mathbb{1} \otimes H$
- b) $(1,2,3,4) = (\pi_B, \pi_A, \mathbf{k}_A, \mathbf{k}_B)$, $\mathcal{U} = H \otimes \sigma_z \otimes \sigma_x \otimes \sigma_z H$
- c) $(1,2,3,4) = (\mathbf{k}_A, \mathbf{k}_B, \pi_B, \pi_A)$, $\mathcal{U} = \sigma_z H \otimes \sigma_x \otimes \mathbb{1} \otimes H$.

In the following we refer to these expressions depending on the logical operation we will consider. Let's now examine the most relevant measurements performed in this experiment.

Single qubit rotations. In the one-way model a three-qubit linear cluster state is sufficient to realize arbitrary single qubit rotations [12, 13], hence this operation may be implemented through three different steps and single qubit measurements. According to the measurement basis for a generic qubit j , $|\varphi_\pm\rangle_j = \frac{1}{\sqrt{2}}(|0\rangle_j \pm e^{-i\varphi}|1\rangle_j)$, we define $s_j = 0$ ($s_j = 1$) when the $|\varphi_+\rangle_j$ ($|\varphi_-\rangle_j$) outcome is obtained. With the four-qubit cluster expressed in the computational basis the following procedure must be performed (see fig. 1(a)):

I: A three-qubit linear cluster is generated by measuring the first qubit in the basis $\{|0\rangle_1, |1\rangle_1\}$. The input logical qubit $|\chi_{in}\rangle$ is then encoded in qubit 2. If the outcome of the first measurement is $|0\rangle_1$ then $|\chi_{in}\rangle = |+\rangle$, otherwise $|\chi_{in}\rangle = |-\rangle$.

II: Measuring qubit 2 in the basis $|\alpha_\pm\rangle_2$, with α corresponding to a particular value of φ , the computational qubit (now encoded in qubit 3) is transformed into $|\chi'\rangle = (\sigma_x)^{s_2} H R_z(\alpha) |\chi_{in}\rangle$, with $R_z(\alpha) = e^{-\frac{i}{2}\alpha\sigma_z}$.

III: Measurement of qubit 3 in the basis $|\beta_\pm\rangle_3$ (if $s_2 = 0$) or $|\beta_\pm\rangle_3$ (if $s_2 = 1$) leaves the last

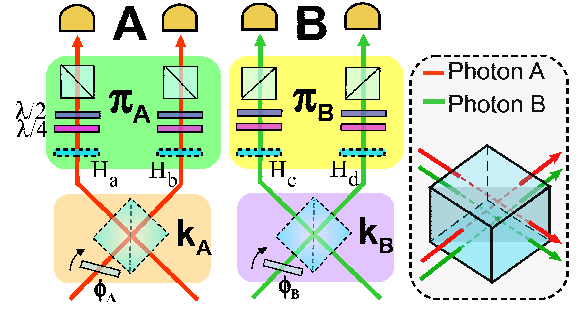


FIG. 2: Measurement setup for photons A and B. Momentum qubits \mathbf{k}_A and \mathbf{k}_B are measured by phase shifters (ϕ_A , ϕ_B) and a common 50:50 BS. Polarization qubits π_A and π_B are measured by $\lambda/4$, $\lambda/2$ waveplate and polarizing beam splitters PBS's. Hadamard gates $H_{a,b,c,d}$ are realized by HW plates. Dashed lines for $H_{a,b,c,d}$ and BS indicate that these devices can be inserted or not in the setup depending on the particular measurement (see text for details). Inset: spatial mode matching on the BS.

qubit in the state $|\chi_{out}\rangle = (\sigma_x)^{s_3} H R_z(\beta) [(-1)^{s_2} \beta] |\chi'\rangle = \sigma_x^{s_3} \sigma_z^{s_2} R_x(\beta) R_z(\alpha) |\chi_{in}\rangle$, with $R_x(\beta) = e^{-\frac{i}{2}\beta\sigma_x}$.

In this way, by suitable choosing the values of α and β , we can perform any arbitrary single qubit rotation $|\chi_{in}\rangle \rightarrow R_x(\beta) R_z(\alpha) |\chi_{in}\rangle$ [17] up to Pauli errors ($\sigma_x^{s_3} \sigma_z^{s_2}$), that can be corrected by proper feed-forward operations [4]. In our case we applied this procedure by considering as output qubit either the polarization or momentum of photon B, demonstrating the QC equivalence of the two degrees of freedom. This corresponds to respectively choose the order a) or b) for the physical qubits.

The measurement apparatus is sketched in fig. 2. The \mathbf{k} modes corresponding to photons A or B, are respectively matched on the up and down side of a common symmetric beam splitter (BS) (see inset), which can be also finely moved in the vertical direction such that one or both photons don't pass through it.

Polarization analyses are performed by standard π tomographic apparatus ($\lambda/4$, $\lambda/2$ and polarizing beam splitter PBS), while two HW oriented at 22.5° (H_a and H_b in fig. 2) are inserted in photon A modes. They will be used together with the $\lambda/4$'s in order to transform the $\{|\varphi_+\rangle_{\pi_A}, |\varphi_-\rangle_{\pi_A}\}$ states into linearly polarized states. Two thin glass plates before the BS allow to set the basis of momentum measurement for each photon.

Let's consider ordering a). The output state, encoded in the polarization of photon B, can be written in the laboratory basis as

$$|\chi_{out}\rangle_{\pi_B} = (\sigma_z)^{s_3} (\sigma_x)^{s_2} H R_x(\beta) R_z(\alpha) |\chi_{in}\rangle, \quad (3)$$

where the H gate derives from the change between the computational and laboratory basis. This also implies that the actual measurement bases are $|\pm\rangle_{\mathbf{k}_B}$ for the momentum of photon B and $|\alpha_\pm\rangle_{\mathbf{k}_A}$ for the momentum of

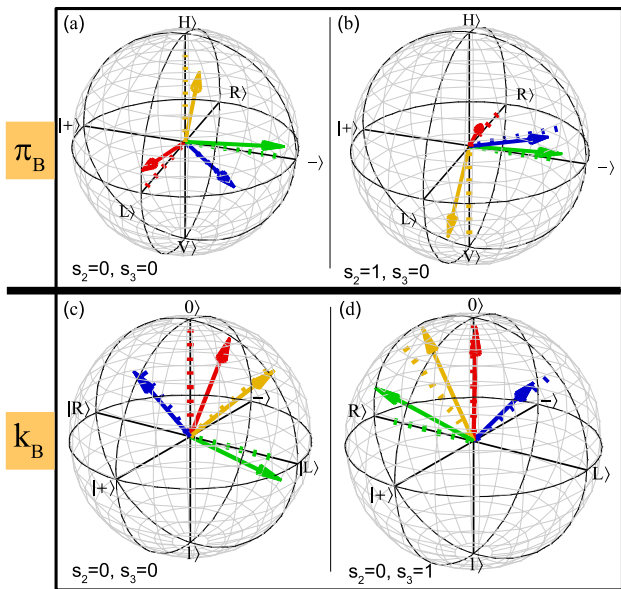


FIG. 3: Polarization (π_B) and momentum (\mathbf{k}_B) output Bloch vectors of single qubit rotations. The experimental results (arrows) are shown with their projections on theoretical directions (dashed lines). Arrow colours correspond to different values of α and β (see table I).

	α	β	F ($s_2 = s_3 = 0$)	F ($s_2 = 1, s_3 = 0$)	Colour
π_B	0	$\pi/2$	0.908 ± 0.006	0.928 ± 0.013	orange
	$-\pi/2$	0	0.942 ± 0.004	0.902 ± 0.007	red
	$-\pi/2$	$\pi/2$	0.913 ± 0.005	0.904 ± 0.010	green
	$-\pi/2$	$-\pi/4$	0.942 ± 0.006	0.955 ± 0.012	blue
	$\alpha(\beta = 0)$		F ($s_2 = s_3 = 0$)	F ($s_2 = 0, s_3 = 1$)	Colour
\mathbf{k}_B	0		0.961 ± 0.003	0.971 ± 0.003	red
	$\pi/2$		0.879 ± 0.006	0.895 ± 0.005	green
	$\pi/4$		0.998 ± 0.005	0.961 ± 0.006	orange
	$-\pi/4$		0.833 ± 0.007	0.956 ± 0.006	blue

TABLE I: Polarization (π_B) and momentum (\mathbf{k}_B) experimental fidelities (F) of single qubit rotation output states for different values of α and β . Each datum is obtained by the measurements of the different Stokes parameters, each one lasting 10 sec. Colours in the last column correspond to those shown in fig. 3.

photon A. The measurement basis on the third qubit (π_A) depends, according to the one-way model, on the results of the measurement on the second qubit (\mathbf{k}_A). Note that in our scheme this simply corresponds to measure it in the bases $|\beta_{\pm}\rangle_{\pi_A}$ or $|-\beta_{\pm}\rangle_{\pi_A}$ depending on the BS output mode (i.e. $s_2 = 0$ or $s_2 = 1$). This is a direct consequence of the possibility to encode two qubits (\mathbf{k}_A and π_A) in the same photon. As a consequence, differently from the case of four-photon cluster states, in this case active feed-forward measurements (e.g. adopting Pockels cells) are not required, while Pauli errors corrections are in any case necessary for deterministic QC.

In fig. 3(a) the results obtained in the case $s_2 = s_3 = 0$ (i.e. when the computation proceeds without errors) with $|\chi_{in}\rangle = |+\rangle$ are given. We report on the Bloch sphere the experimental output qubits and their projections on the theoretical state $HR_x(\beta)R_z(\alpha)|+\rangle$ for different values of α and β . The corresponding fidelities are given in table I. We also performed the tomographic analysis on the output qubit π_B for all the possible combinations of s_2 and s_3 and for input qubit $|\chi_{in}\rangle = |\pm\rangle$. In all the cases we obtained an average value of fidelity $F \approx 0.9$. As an example, we show in fig 3(b) the case $s_2 = 1, s_3 = 0$ ($|\chi_{in}\rangle = |+\rangle$). The high values of the fidelity obtained in these measurements represent the necessary condition to implement efficient active feed-forward corrections.

By considering ordering b) the same computation can be performed with output state $|\chi_{out}\rangle_{\mathbf{k}_B}$ encoded in the linear momentum of photon B, whose explicit expression in the laboratory basis is

$$|\chi_{out}\rangle_{\mathbf{k}_B} = (\sigma_z)^{s_3} (\sigma_x)^{s_2} \sigma_z HR_x(\beta)R_z(\alpha)|\chi_{in}\rangle. \quad (4)$$

By the apparatus of fig. 2 we measured $|\chi_{out}\rangle_{\mathbf{k}_B}$ by choosing different values of α (corresponding in the laboratory to the polarization basis $|\alpha_{\mp}\rangle_{\pi_A}$) and $\beta = 0$ (corresponding in the laboratory to the momentum basis $|-\beta_{\pm}\rangle_{\mathbf{k}_A}$), while the first qubit (π_B) was always measured in the basis $|\pm\rangle_{\pi_B}$. In this case only H_a and H_b Hadamard gates are inserted. The complete single qubit tomography on \mathbf{k}_B requires the measurement of the σ_x, σ_y operators, by proper setting of phase ϕ_B , and σ_z , performed by removing the BS on photon B.

Fig. 3(c) shows the results obtained for different output qubits, for $s_2 = s_3 = 0$ and $|\chi_{in}\rangle = |+\rangle$. The corresponding fidelities are given table I. Also in this case we performed the \mathbf{k}_B tomographic analysis for all the possible values of s_2 and s_3 and of the input qubit, obtaining in average $F > 0.9$. The case $s_2 = 0, s_3 = 1$ is shown in fig. 3(d) with fidelities given in table I.

C-NOT gate for equatorial qubits. Nontrivial two-qubit operations, such as the C-NOT gate, can be realized by the four-qubit horseshoe (180° rotated) cluster state (see fig. 1b)), whose explicit expression is equal to $|\Phi_4^{\text{lin}}\rangle$. By simultaneously measuring qubits 1 and 4, it's possible to implement the logical circuit shown in fig. 1(b). In the computational basis the input state is $|+\rangle_c \otimes |+\rangle_t$ (c =control, t =target), while the output state, encoded in qubits 2 (control) and 3 (target), is $|\Psi_{out}\rangle = H_t C\text{-NOT}(\mathcal{O}|+\rangle_c \otimes R_z(\alpha)|+\rangle_t)$ (for $s_1 = s_4 = 0$). In the above expression we have $\mathcal{O} = \mathbb{1}$ ($\mathcal{O} = H$) when qubit 1 is measured in the basis $\{|0\rangle_1, |1\rangle_1\}$ ($|\pm\rangle_1$). Qubit 4 is measured in the basis $|\alpha_{\pm}\rangle_4$. It is worth noting that this circuit realizes the C-NOT gate (up to the Hadamard H_t) for arbitrary equatorial target qubit and control qubit $|0\rangle, |1\rangle$ or $|\pm\rangle$ depending on the measurement basis of qubit 1.

The experimental realization of this gate is performed by adopting ordering c). In this case the control output

\mathcal{O}	α	Control output	$F(s_4 = 0)$	$F(s_4 = 1)$
H	$\pi/2$	$s_1 = 0 \rightarrow 1\rangle_c$	0.965 ± 0.004	0.975 ± 0.004
		$s_1 = 1 \rightarrow 0\rangle_c$	0.972 ± 0.004	0.973 ± 0.004
	$\pi/4$	$s_1 = 0 \rightarrow 1\rangle_c$	0.995 ± 0.008	0.902 ± 0.012
		$s_1 = 1 \rightarrow 0\rangle_c$	0.946 ± 0.010	0.945 ± 0.009
\mathcal{O}	α	Control output	$F(s_1 = s_4 = 0)$	$F(s_1 = 0, s_4 = 1)$
$\mathbb{1}$	$\pi/2$	$ 0\rangle_c \equiv \ell\rangle_{\mathbf{k}_B}$	0.932 ± 0.004	0.959 ± 0.003
		$ 1\rangle_c \equiv r\rangle_{\mathbf{k}_B}$	0.941 ± 0.005	0.940 ± 0.005
	$\pi/4$	$ 0\rangle_c \equiv \ell\rangle_{\mathbf{k}_B}$	0.919 ± 0.007	0.932 ± 0.007
		$ 1\rangle_c \equiv r\rangle_{\mathbf{k}_B}$	0.878 ± 0.009	0.959 ± 0.006

TABLE II: Experimental fidelity (F) of C-NOT gate output target qubit for different value of α and \mathcal{O} .

qubit is encoded in the momentum \mathbf{k}_B , while the target output is encoded in the polarization π_B . In the actual experiment we inserted H_c and H_d on photon B to compensate H_t , (while H_a and H_b were removed, see fig. 2). The output state in the laboratory basis is then

$$|\Psi_{out}\rangle = (\Sigma)^{s_4} \sigma_x^{(c)} C-NOT(\mathcal{O}\sigma_z^{s_1}|+\rangle_c \otimes R_z(\alpha)|+\rangle_t), \quad (5)$$

where all the possible measurement outcomes of qubits 1 and 4 are considered. The Pauli errors are $\Sigma = \sigma_z^{(c)} \sigma_z^{(t)}$, while the matrix $\sigma_x^{(c)}$ is due to the changing between computational and laboratory basis. Table II shows the experimental fidelities of the target qubit corresponding to the measurement of the output control qubit in the basis $\{|0\rangle, |1\rangle\}$.

The results of our experiment indicate that a two-photon four-qubit cluster state, which realizes the full entanglement of two photons through two degrees of freedom (in our case polarization and linear momentum), represents a basic resource for one-way QC. Indeed, any kind of single qubit rotations on the Bloch sphere can be realized by these states with high fidelity. These transformations were performed at average repetition rates of ~ 1 kHz by equivalently using polarization or momentum as output qubit. The two photon approach allows to implement this algorithm without the need of active devices for feed-forward measurements, as demonstrated in the present work in the case of polarization output qubit. One-way QC requires highly efficient active feed-forward corrections at the end of the process [4]. The high fidelity of the output states obtained in this work, even in presence of Pauli errors, is a necessary condition for deterministic QC. By using the same cluster states, we also realized a C-NOT gate for target qubits located in the equatorial plane of the Bloch sphere. Other two qubit algorithms, such as Grover's algorithm and C-Phase gate, were also implemented by us with the same source. Results will be reported elsewhere.

More complex algorithms could be realized by increasing the number of entangled qubits in the state. For instance, six qubits are necessary to implement a C-

NOT gate operating over the entire Bloch sphere. In our scheme more qubits could be entangled by using different degrees of freedom, such as time-energy or exploiting the continuous k-mode emission within the SPDC cone of a type I crystal, and/or increasing the number of photons. For example eight-qubit four-photon cluster state cloud be generated by linking together two $|C_4\rangle$ states by a proper CP gate. These different approaches are at the moment under investigation.

Thanks are due to Fabio Sciarrino for useful discussions and Marco Barbieri for his contribution in planning the experiment. This work was supported by the PRIN 2005 of MIUR (Italy).

Note added- While we were completing the experiment another work concerning one-way QC with two-photon four-qubit cluster states appeared [14].

* URL: <http://quantumoptics.phys.uniroma1.it/>

- [1] R. Raussendorf and H. J. Briegel, Phys. Rev. Lett. **86**, 5188 (2001).
- [2] N. Kiesel, C. Schmid, U. Weber, G. Tóth, O. Gühne, R. Ursin, and H. Weinfurter, Phys. Rev. Lett. **95**, 210502 (2005).
- [3] P. Walther, K. J. Resch, T. Rudolph, E. Schenck, H. Weinfurter, V. Vedral, M. Aspelmeyer, and A. Zeilinger, Nature **434**, 169 (2005).
- [4] R. Prevedel, P. Walther, F. Tiefenbacher, P. Böhi, R. Kaltenbaek, T. Jennewein, and A. Zeilinger, Nature **445**, 65 (2007).
- [5] A. Cabello, Phys. Rev. Lett. **95**, 210401 (2005).
- [6] V. Scarani, A. Acin, E. Schenck, and M. Aspelmeyer, Phys. Rev. A **71**, 042325 (2005).
- [7] G. Vallone, E. Pomarico, P. Mataloni, F. De Martini, and V. Berardi, Phys. Rev. Lett. **98**, 180502 (2007).
- [8] E. Knill, R. Laflamme, and G. J. Milburn, Nature **409**, 46 (2001).
- [9] M. Barbieri, C. Cinelli, P. Mataloni, and F. De Martini, Phys. Rev. A **72**, 052110 (2005).
- [10] M. Barbieri, F. De Martini, P. Mataloni, G. Vallone, and A. Cabello, Phys. Rev. Lett. **97**, 140407 (2006).
- [11] C. Cinelli, M. Barbieri, R. Perris, P. Mataloni, and F. De Martini, Phys. Rev. Lett. **95**, 240405 (2005).
- [12] R. Raussendorf, D. E. Browne, and H. J. Briegel, Phys. Rev. A **68**, 022312 (2003).
- [13] M. S. Tame, M. Paternostro, M. S. Kim, and V. Vedral, Phys. Rev. A. **72**, 012319 (2005).
- [14] K. Chen, C.-M. Li, Q. Zhang, Y.-A. Chen, A. Goebel, S. Chen, A. Mair, and J.-W. Pan (2007), [[arXiv:0705.0174](https://arxiv.org/abs/0705.0174)].
- [15] The state (1) is equivalent to that generated in [7] up to single qubit transformations.
- [16] The state $|\Phi_4^{in}\rangle$ is obtained by preparing a chain of qubits all prepared in the state $|+\rangle$ and then applying the gate $CP = |0\rangle\langle 0| \otimes \mathbb{1} + |1\rangle\langle 1| \otimes \sigma_z$ for each link.
- [17] Three sequential rotations are necessary to implement a generic $SU(2)$ matrix but only two, namely $R_x(\beta)R_z(\alpha)$, are sufficient to rotate the input state $|\chi_{in}\rangle = |\pm\rangle$ into a generic state